Computers and Chemical Engineering 34 (2010) 508–517

Contents lists available at ScienceDirect

Computers and Chemical Engineering

journal homepage: www.elsevier.com/locate/compchemeng

Repetitive control and online optimization of Catofin propane process

Wangyun Won [a], Kwang Soon Lee [a,*], Seokho Lee [b], Chansul Jung [b]

[a] Department of Chemical and Biomolecular Engineering, Sogang University, 1 Shinsoodong, Mapogu, Seoul 121-742, South Korea
[b] Samsung Engineering Co. Ltd., 2 Dogokdong, Gangnamgu, Seoul 135-856, South Korea

ARTICLE INFO

Article history:
Received 26 March 2009
Received in revised form
23 December 2009
Accepted 29 December 2009
Available online 14 January 2010

Keywords:
Catofin process
Online optimization
Repetitive control
Adiabatic fixed-bed reactor

ABSTRACT

The Catofin propane process is an emerging industrial process for propylene production through dehydrogenation of propane. It is composed of multiple adiabatic fixed-bed reactors which undergo cyclic operations where propane dehydrogenation and catalyst regeneration alternate over roughly 10-min period for each. One of the major concerns in the operation of the Catofin process is maintaining the reactor at an optimum condition while overcoming gradual catalyst deactivation. Addressing this issue, an online optimization of the Catofin process combined with a repetitive control has been investigated. The optimizer computes optimum initial bed temperatures for dehydrogenation and optimum air flow rate for regeneration, and the repetitive controller performs cycle-wise feedback action during regeneration to attain the target bed temperatures at the terminal time of the regeneration period. Numerical studies have shown that the proposed online optimizing control system performs satisfactorily coping with the catalyst deactivation and other disturbances.

1. Introduction

Advanced control and online optimization are now accepted as an essential process intensification technology that can create an additional profit in process industries wherever they are applicable. During the past two decades or more, there have been numerous industrial projects for advanced process control alone or integrated with online optimization as reviewed in Qin and Badgwell (2003). Such projects have typically proceeded for continuous processes with linear MPC only or cascaded by online steady state optimization. While the continuous process with steady state operation represents the majority of the chemical processes, repetitive continuous process, which is characterized by the periodic reference trajectory and/or disturbance, and also non-continuous processes such as batch and semi-batch processes take an important part. Such processes are run under unceasing dynamics, which renders conventional advanced control and online optimization techniques to show limitations in the performance. In this research, a repetitive process called the Catofin propane process (ABB, 2008) has been addressed and an advanced control technique combined with online optimization that exploits the unique nature of the Catofin process has been investigated.

The Catofin propane process is an emerging process for propylene production through propane dehydrogenation. The process was developed by Houdry Co. in the late 1980s with the advancement of the Cr_2O_3/Al_2O_3 catalyst that had long been used for butenes production from butanes (Bhasin, McCaina, Vora, Imai, & Pujad, 2001). As of year 2009, a plant with 455,000 MT/yr of propylene production is being under commercial operation and another one with 650,000 MT/yr capacities will be constructed by 2011 in Saudi Arabia (Reuters, 2008). The operation of the Catofin process consists of repetition of four sequential modes: propane dehydrogenation (DH), purge, catalyst regeneration (RG, coke burning), and evacuation. DH and RG are major operation modes that take around 10 min each; purge and evacuation are the preparative modes which finish in two to three minutes each. One of the major concerns in the operation of the Catofin process is how to reach a desired cyclic steady state with a minimum transient and maintain the process at an optimum state coping with the catalyst deactivation and other disturbances. This concern is a typical advanced control and online optimization problem, but the fact that the Catofin process is under a cyclic operation makes the problem unique.

In chemical engineering, the simulated moving bed (SMB) and pressure swing adsorption (PSA) are typical repetitive processes besides the Catofin process. For such processes, the operation is performed under a cyclic steady state and the cyclic steady state optimization should be done instead of the steady state optimization. Also there is an opportunity to greatly improve the control performance through cycle-wise feedback using the technique of the so-called repetitive control (Hara, Yamamoto, Omata, & Nakano, 1988; Lee, Natarajan, & Lee, 2001). So far, repetitive control has been most actively, though not widely, applied to the SMB process as a purity regulator (Natarajan & Lee, 2000) and an optimizing con-

* Corresponding author. Tel.: +82 2 705 8477; fax: +82 2 3272 0319.
E-mail address: kslee@sogang.ac.kr (K.S. Lee).

0098-1354/$ – see front matter © 2010 Elsevier Ltd. All rights reserved.
doi:10.1016/j.compchemeng.2009.12.011

troller (Abel, Mazzotti, Erdem, Morari, & Morbidelli, 2004; Erdem et al., 2004). Different techniques for optimization of the SMB process subject to the cyclic steady state constraint have also been studied (Kawajiri & Biegler, 2006). On the other hand, it seems that only the cyclic steady state optimization has been researched for the PSA process (Jiang, Biegler, & Fox, 2003; Jiang, Fox, & Biegler, 2004) and no study has been reported on repetitive control or optimization of the Catofin process according to authors' survey.

In this study, an online optimizing control system for the Catofin propane process has been proposed and investigated numerically. The optimizing control system is composed of two tiers, a repetitive controller cascaded by an online optimizer. Repetitive control is put into an action during the RG steering the bed temperatures at two axial positions to reach the target values at the terminal time of the RG period. The open-loop operation with only a state estimation is conducted during the DH. The optimizer calculates the optimum target values for the bed temperatures and the RG air flow rate under a cyclic steady state. Both repetitive control and online optimization were constructed on the basis of a first principle reactor model reduced to a set of ordinary differential equations (ODEs) using the cubic spline collocation method (CSCM) (Yun & Lee, 2007). For the repetitive control, the model is linearized before the start of each RG cycle around the operating trajectories in the previous cycle. The performance of the proposed optimizing control scheme has been investigated numerically.

2. Process description

Fig. 1 shows a simplified process flow diagram of the Catofin propane process. It consists of multiple parallel adiabatic fixed-bed reactors that contain Cr_2O_3/Al_2O_3 catalyst, where the DH of propane and RG of catalyst are carried out alternatively over roughly 10-min period each with short periods of purging and evacuation operations in-between. In order to produce propylene at a constant rate, the operations of the multiple reactors are exquisitely scheduled so that the DH and RG incessantly take place at the same number of reactor beds.

The DH reaction is endothermic and produces a significant amount of coke. The bed temperatures are decreased and the catalyst loses activity by coke deposit and chromium reduction from Cr (IV) to Cr (III) during this period. The RG reaction is coke burning by hot air and both the bed temperatures and catalyst activity are recovered under the oxidizing condition. The temperature of the RG air is controlled by combusting a small amount of natural gas with the RG air in addition to the heat exchange in the reactor charge heater (see Fig. 1). The reaction temperature and pressure for the DH are around 600 °C and in the range of 0.2–0.5 bar, respectively (Bhasin et al., 2001). The catalyst is known to have two years of life time and gradually loses the activity as the number of active sites is diminished by surface migration and agglomeration of Cr_2O_3 (Nijhuis, Tinnemans, Visser, & Weckhuysen, 2004).

It is true that the reaction rates change within the DH and RG periods due to the varying catalyst oxidation state and coke deposit. Such detailed phenomena are neglected in this study and the following apparent reaction kinetics proposed by Kim, Lee, and Song (1980) for the propane DH and Mickley, Nestor, and Gould (1965) and Pena, Monzon, and Santamaria (1993) for the coke combustion were assumed:

$$\begin{cases} C_3H_8 \underset{r_2}{\overset{r_1}{\rightleftharpoons}} C_3H_6 + H_2 \quad C_3H_6 \xrightarrow{r_3} 3C + 3H_2 \\ C_3H_8 + C_3H_6 \xrightarrow{r_4} 2CH_4 + C_2H_6 + 2C \end{cases} \tag{1}$$

$$C + O_2 \xrightarrow{r_5} CO_2 \tag{2}$$

The rate constants are given in Table 1, which were slightly adjusted from the original values (Kim et al., 1980; Mickley et al., 1965; Pena et al., 1993) to more closely fit the conversion and yield of the real process (ABB, 2008).

To prepare for the switching from DH to RG, purging combustable gases in the reactor bed is needed. Reversely, for the switching from RG to DH, evacuation to lower the bed pressure should be conducted. The purge and evacuation can be considered to reset the system. However, it is not true because the coke deposit and the bed temperature are transferred from DH to RG and also RG to DH, respectively, and the Catofin process can be classified as a repetitive process instead of a batch process.

It is assumed that the bed temperatures are measured at $z = 0.2$, 0.4, 0.6, 0.8, and 1.0, respectively, where z represents the normalized axial distance of the reactor bed. The product gas compositions are assumed to be available as the time average values over the DH and RG periods each with one cycle of measurement delay. It is also assumed that the RG is conducted under feedback control while the

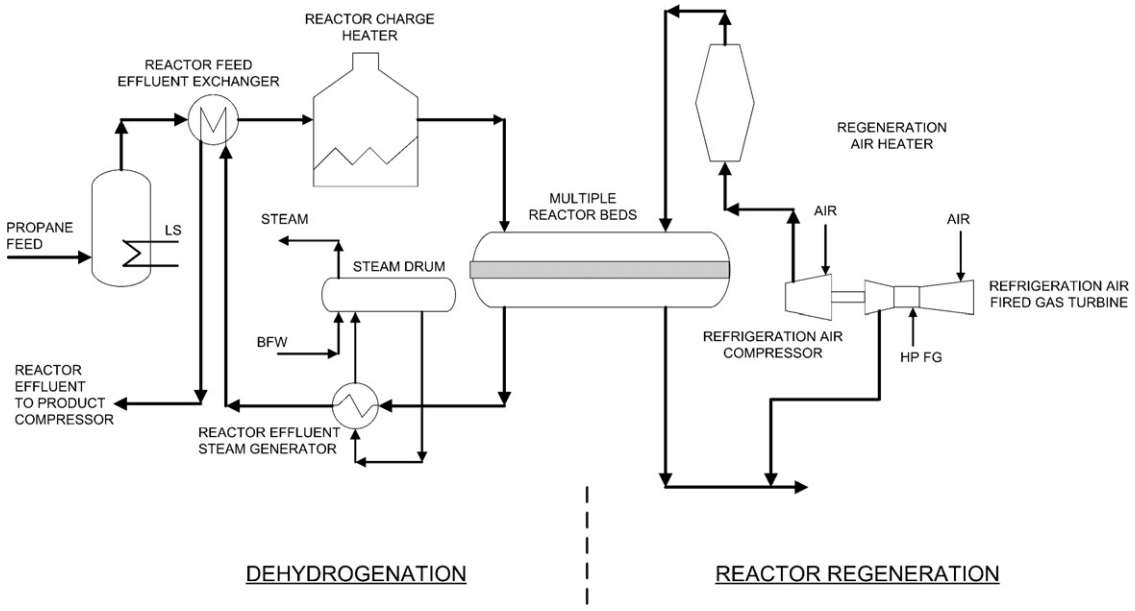

Fig. 1. Process flow diagram of the Catofin propane process.

Table 1
Parameters and normal operating conditions for the Catofin reactor model.

Constants	Bed length = 1.5 (m), bed diameter = 5.7 (m) c_{pc} = 0.80 (kJ/kg K), $\rho_c = 8 \times 10^2$ (kg/m^3) c_{pg} = 3.71 for DH, 5.66 (kJ/kg K) for RG D = 1.7 for DH, 0.76 (m^2/min) for RG k_B = 1.982 (kJ/min m K), T_{ref} = 25 (°C) R = 8.3462 (kJ/kmol K), DH and RG periods = 9 min each
Normal operating condition for DH	Inlet temp = 650 °C, propane flow = 56.8 (kmol/min), P = 0.5 (atm)
Reaction rates (kmol/kg-cat min) for DH	$r_1 = k_1[C_3H_8]\,RT$, $k_1 = 3.126 * 10^7 \exp(-47{,}100/RT)$ $r_2 = k_2[C_3H_8][H_2]\,R^2T^2$, $k_2 = 9.70 * 10^{-3} \exp(-12{,}800/RT)$ $r_3 = k_3[C_3H_6]\,R^2T^2$, $k_3 = 8.407 * 10^9 \exp(-62{,}900/RT)$ $r_4 = k_4[C_3H_8][C_3H_6]\,R^2T^2$, $k_4 = 9.498 * 10^5 \exp(-47{,}800/RT)$ In the above equations, T in [K]
Normal operating condition for RG	Inlet temp. = 690 °C, air flow = 103.4 (kmol/min), P = 2.0 (atm)
Reaction rate for RG	$r_5 = k_5[C][O_2]\,RT$, $k_5 = 4.129 * 10^3 \exp(-25{,}575/RT)$, T in [K]

DH is carried out in an open loop state under a constant propane flow rate; both RG and DH take 9 min each and purge and evacuation operations are finished instantaneously. The control objective during the RG is to steer the bed temperatures at z = 0.2 and 0.4 to the target values provided by the optimizer using the RG air temperature as a manipulating variable (MV). The RG air flow rate is not separately manipulable for the individual reactors in the real process and was not considered as an MV. Instead, the RG air flow rate was chosen as a decision variable for the optimizer together with the bed temperature target values.

3. Reactor modelling

3.1. Mass and energy balances

In an adiabatic fixed-bed reactor, radial distribution of the concentrations and temperatures can be neglected. Under this assumption, the component mass and energy balance equations are written as (Froment & Bischoff, 1990)

$$\frac{\partial C_i}{\partial t} = \left(\frac{D}{L^2}\right)\frac{\partial^2 C_i}{\partial z^2} - \left(\frac{v_g}{L}\right)\frac{\partial C_i}{\partial z} + \left(\frac{1-\varepsilon}{\varepsilon}\right)\rho_c \bar{r}_i$$
$$\frac{\partial C_c}{\partial t} = \rho_c \bar{r}_c \qquad (3)$$
$$\text{I.C.}: \quad C_i = C_i^I(z) \ \text{at} \ t = 0$$
$$\text{B.C.}: \quad C_i = C_i^0(t) \ \text{at} \ z = 0, \quad \frac{dC_i}{dz} = 0 \ \text{at} \ z = L_f = 5$$

$$\frac{\partial T}{\partial t} = \left(\frac{k_B}{\rho_c c_{pc} L^2}\right)\frac{\partial^2 T}{\partial z^2} - \left(\frac{\varepsilon}{1-\varepsilon}\right)\left(\frac{\rho_g c_{pg} v_g}{\rho_c c_{pc} L}\right)\frac{\partial T}{\partial z} - \left(\frac{1}{c_{pc}}\right)\sum_j \Delta H_j r_j \qquad (4)$$
$$\text{I.C.}: \quad T = T_o(z) \ \text{at} \ t = 0$$
$$\text{B.C.}: \quad T = T_o(t) \ \text{at} \ z = 0, \quad \frac{dT}{dz} = 0 \ \text{at} \ z = L_f = 5$$

where $\bar{r}_i$ and C_i represent the rate of generation (kmol/kg-cat min) and concentration (kmol/m^3) of component i, which refers to C_3H_8, C_3H_6, H_2, CH_4, C_2H_6 for DH operation, and CO_2, O_2 for RG operation, respectively; $\bar{r}_c$ and C_c represent the rate of generation (kmol/kg-cat min) and concentration (kmol/m^3) of coke, respectively; r_j refers to the rate of the jth reaction; z denotes the normalized axial distance. Note that $\bar{r}_c$ for DH is different from $\bar{r}_c$ for RG. Other parameters and variables in the above model equations are given in Table 1.

In the above, the second boundary condition is specified at $z = 5$ instead of $z = 1$ whereas the spatial domain is $z \in (0, 1]$. The reason for this is to more reasonably represent the true phenomenon, $dT/dz \to 0$ as $z \to \infty$, using a condition at a distant axial position, which was named as the far-side boundary condition (Yun & Lee, 2007).

3.2. ODE models by cubic spline collocation method

ODE models for the virtual process and nominal model were derived separately using the CSCM (Yun & Lee, 2007) using ten and five equally spaced collocation points over (0, 1] plus an additional point at $z = 5$, respectively. The resulting ODE models can be concisely written as

$$\frac{d\bar{x}_k^i}{dt} = \bar{f}^i(\bar{x}_k^i, u_k^i), \quad i = \text{DH, RG} \qquad (5)$$

In the above, the subscript k denotes the cycle number; $\bar{x}^{DH}$ represents the state for the DH model, that consists of bed temperatures, concentrations of C_3H_8, C_3H_6, H_2, CH_4, C_2H_6, and C at the internal collocation points; $\bar{x}^{RG}$ is similar to $\bar{x}^{DH}$ except that the concerned chemical components are C and O_2; u denotes the MV and represents the air temperature T^{air} for i = RG and is void for i = DH, respectively.

3.3. Process behaviour under a cyclic steady state

Fig. 2 shows the bed temperature trajectories of the virtual process under a cyclic steady state at the nominal operating condition. The bed temperatures are initially increased as the higher bed temperatures in the fore part of the respective collocation points recede by the gas flow. After a while, however, bed temperatures are decreased by the endothermic reactions as the propane DH proceeds and restored again by the coke combustion during the RG. The amount for the coke deposit changes during this operation are as shown in Fig. 3. The coke generation is larger at the higher temperature positions and vice versa.

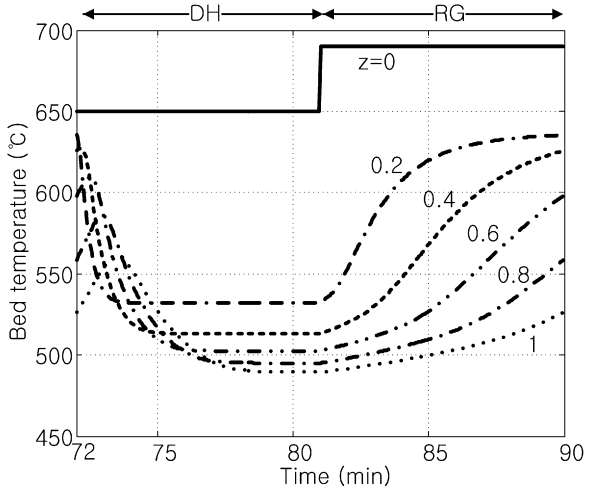

Fig. 2. Bed temperature trajectories at six axial positions under a cyclic steady state.

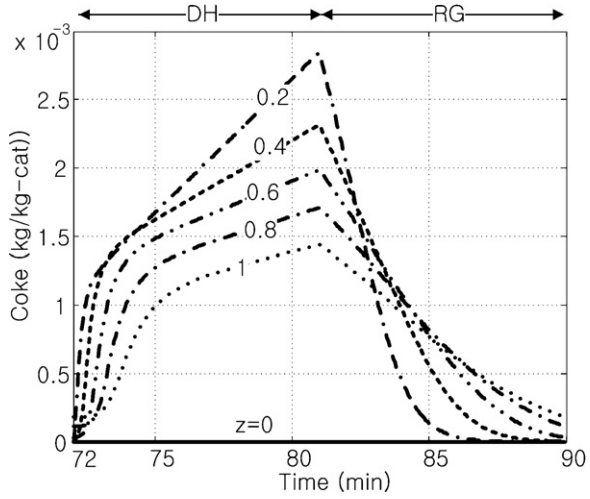

Fig. 3. Trajectories of coke deposit at six axial positions under a cyclic steady state.

The associated propane and propylene concentration trajectories during propane DH are shown in Fig. 4. Over an initial period while the bed temperatures are high, almost complete propane conversion and high propylene yield are obtained at the reactor outlet. As the bed temperatures begin to fall, both the propane conversion and propylene yield decrease. If we scrutinize Fig. 4, it can be seen that the front half of the bed where temperatures are higher than the rear half contribute more than 78.2% of the propylene production. The propane conversion and propylene selectivity averaged over a DH period are 51.5% and 86.2%, respectively.

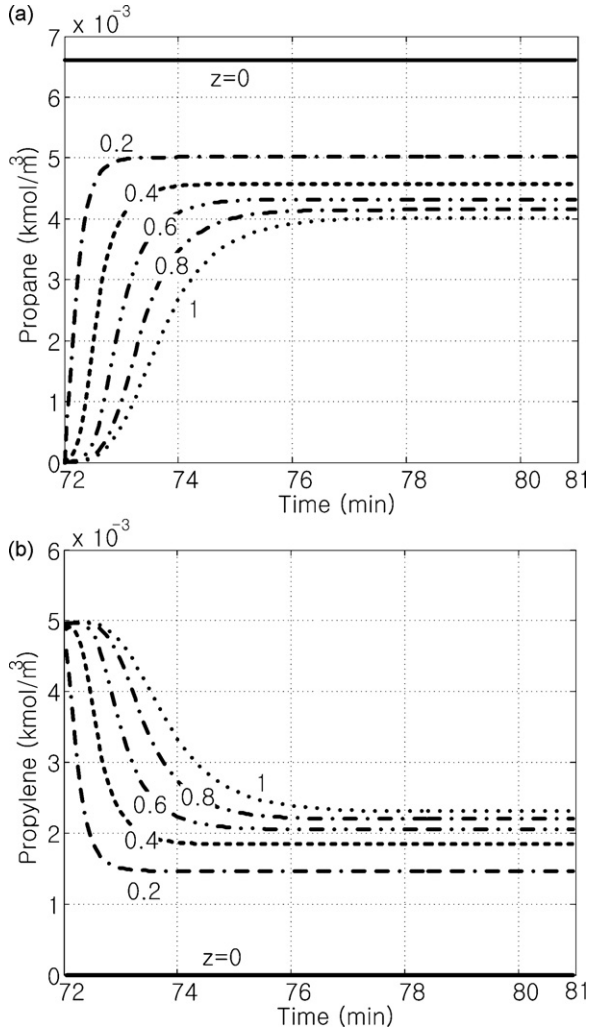

Fig. 4. Trajectories of propane and propylene concentrations under a cyclic steady state.

4. Optimizing control system

4.1. Structure

The optimizing control system consists of three major parts: the online cyclic steady state optimizer, the repetitive controller, and the model parameter estimator. The repetitive controller has a state estimator as its part. Fig. 5 shows the overall structure of the proposed system. The optimizer computes the optimum initial bed temperatures at $z = 0.2$ and 0.4 for the DH operation and the air flow rate for the RG operation using process measurements and the reactor model such that the cost function is minimized. The optimum temperatures are provided to the repetitive controller as the target values and pursued during the RG operation to reach at the terminal time of the period. The model parameter estimator updates key parameters of the reactor model on the basis of the available measurements.

Fig. 6 illustrates the information flow through the state estimators along the operational sequence in more detail. The state estimation continues for the DH as well as RG periods based on the measurements of the bed temperatures and average product gas compositions in the previous cycle. Estimates of the coke deposit and bed temperature at the collocation points are transferred from the DH to RG and also from the RG to DH. The bed temperature estimates can be replaced by the measurement values. Each part of the optimizing control system will be described in more detail.

4.2. Repetitive control

4.2.1. Discrete-time nominal model

We first describe how the discrete-time nominal model for the state estimator and controller design is derived. The forward difference approximation applied to Eq. (5) results in

$$\bar{x}_k^i(t+1) = \bar{g}^i(\bar{x}_k^i(t), u_k^i(t)), \quad i = \text{DH, RG} \tag{6}$$

The output equation can be written as

$$\begin{aligned} \bar{y}_k^i(t) &= V^i \bar{x}_k^i(t), \\ \bar{p}_k^i &= \frac{1}{N}\sum_{n=0}^{N-1} H^i \bar{x}_{k-1}^i(n), \quad i = \text{DH, RG} \end{aligned} \tag{7}$$

where $\bar{y}$ and $\bar{p}$ represent the bed temperatures at $z = 0.2, 0.4, \ldots, 1.0$ and the average product gas composition measured at the end of the DH and RG periods with one cycle of measurement delay, respectively; N denotes the total number of sampling instance during the period of DH (or RG). V is a matrix that extracts the bed temperatures from the state and H is defined in a similar way for the compositions at the bed outlet. Hereafter, let us drop the superscript i for notational simplicity wherever there is no confusion.

The composition equation in Eq. (7) can be rewritten in the form of a state space equation. For this, let us define

$$\bar{p}_k(t+1) \triangleq \frac{1}{N}\sum_{n=0}^{t} H \bar{x}_{k-1}(n)$$

$$\begin{aligned} &w_{1,k}(t) \triangleq \bar{x}_{k-1}(t), \quad w_{2,k}(t) \triangleq \bar{x}_{k-1}(t+1), \ldots \\ &, w_{N,k}(t) \triangleq \bar{x}_{k-1}(t+N-1) = \bar{x}_k(t-1) \end{aligned} \tag{8}$$

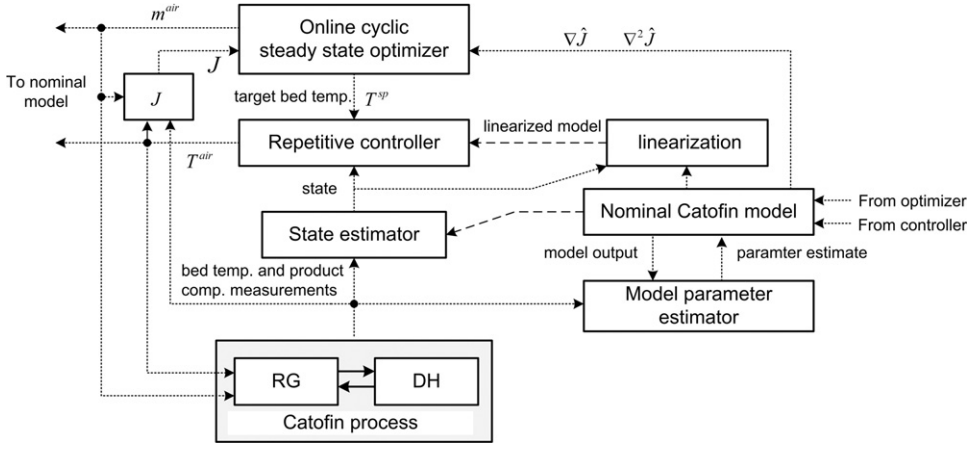

Fig. 5. Structure of the optimizing control system.

$$\bar{w}_k(t) \triangleq \begin{bmatrix} w_{1,k}(t) \\ w_{2,k}(t) \\ \vdots \\ w_{N-1,k}(t) \\ w_{N,k}(t) \end{bmatrix}, \quad M \triangleq \begin{bmatrix} 0 & I & 0 & \cdots & 0 \\ 0 & 0 & I & \cdots & 0 \\ \vdots & \vdots & \ddots & \vdots & \vdots \\ 0 & 0 & 0 & \cdots & I \\ 0 & 0 & 0 & \cdots & 0 \end{bmatrix},$$

$$J \triangleq \begin{bmatrix} 0 \\ 0 \\ \vdots \\ 0 \\ I \end{bmatrix}, \quad \bar{J} \triangleq \begin{bmatrix} I & 0 & \cdots & 0 & 0 \end{bmatrix}$$

Then the associated state transition equations are recast to

$$\begin{aligned} \bar{x}_k(t+1) &= \bar{g}(\bar{x}_k(t), u_k(t)) \\ \bar{w}_k(t+1) &= J\bar{x}_k(t) + M\bar{w}_k(t) \\ \bar{p}_k(t+1) &= \bar{p}_k(t) + \frac{1}{N} H\bar{J}\,\bar{w}_k(t) \end{aligned}, \tag{9}$$

The resulting model equation can be rewritten in the following simplified form:

$$\begin{aligned} x_k(t+1) &= g(x_k(t), u_k(t)) \\ y_k(t) &= c(t)x_k(t) \end{aligned} \tag{10}$$

where

$$\begin{aligned} &x_k(t) \triangleq \begin{bmatrix} \bar{x}_k(t) \\ \bar{w}_k(t) \\ \bar{p}_k(t) \end{bmatrix}, \\ &y_k(t) = \bar{y}_k(t) \text{ and } c(t) = \begin{bmatrix} V & 0 & 0 \end{bmatrix} \quad \text{for } t = 1, \ldots, N-1 \\ &y_k(N) = \begin{bmatrix} \bar{y}_k(N) \\ \bar{p}_k(N) \end{bmatrix} \text{ and } c(N) = \begin{bmatrix} V & 0 & 0 \\ 0 & 0 & I \end{bmatrix} \end{aligned} \tag{11}$$

Note that Eqs. (10) and (11) holds for DH and RG separately.

4.2.2. Control algorithm for RG operation

The repetitive control conducts cycle-wise integral control action. To facilitate the construction of the control law, it is convenient to transform Eq. (10) to a state space model with $\Delta u_k(t) \triangleq u_k(t) - u_{k-1}(t)$ and $y_k(t)$ as the input and output variables, respectively. Linearization of Eq. (10) around the trajectories of the process variables in the $k-1$th cycle yields

$$\begin{aligned} \Delta x_k(t+1) &= A_{k-1}(t)\Delta x_k(t) + B_{k-1}(t)\Delta u_k(t) \\ y_k(t) &= y_{k-1}(t) + C_{k-1}(t)\Delta x_k(t) \end{aligned} \tag{12}$$

where $\Delta x_k(t) \triangleq x_k(t) - x_{k-1}(t)$; $A_{k-1}(t)$ represents a shorthand notation of $A_{k-1}(u_{k-1}(t), x_{k-1}(t|t))$, and similarly for $B_{k-1}(t)$ and $C_{k-1}(t)$. The control objective is to drive the bed temperatures at $z = 0.2,\ 0.4$ to the respective set points at the terminal time of the RG operation. To achieve this, it will be enough to allow $\Delta u_k(t)$ to change at some selected time moments, i.e., at $t_1(=0), t_2, \ldots, t_{N_p}$ during the RG period instead of changing at every sampling time. By including an input penalty term, the control objective can be

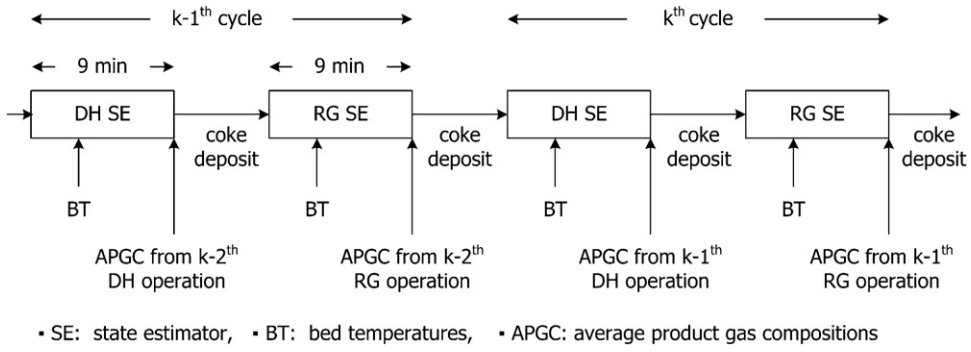

Fig. 6. Information flow along the sequence of operations.

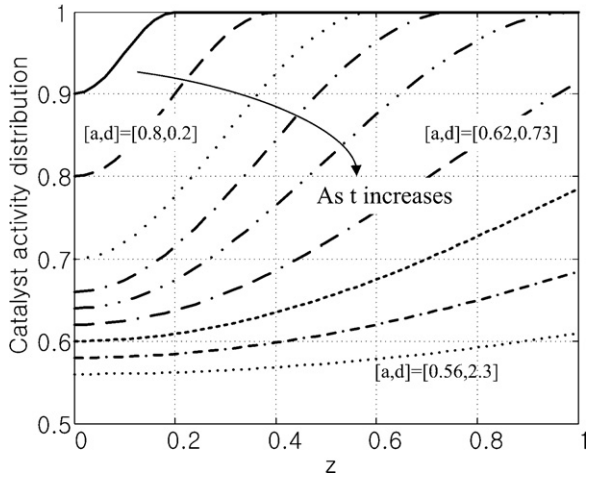

Fig. 7. Sample catalyst activity profiles calculated using Eq. (18).

stated as

$$\min_{\Delta u_k(\bullet)} \left[\left\| T_k^{sp} - \hat{y}_k(N|t_m) \right\|_Q^2 + \sum_{n=m}^{N_P} \left\| \Delta u_k(t_n) \right\|_{R(m)}^2 \right], \quad m = 1, \ldots, N_P$$
$$\text{subject to input constraints} \tag{13}$$

At other occasions than t_m, $m = 1, \cdots, N_P$ $\Delta u(t) = 0$. In the above, $\hat{y}_k(N|t_m)$ represents a prediction of $\hat{y}_k(N)$, the bed temperatures at $z = 0.2$ and 0.4, on the basis of the information up to t_m at the kth cycle; T_k^{sp} denotes the target value of $\hat{y}_k(N)$. $\hat{y}_k(N|t_m)$ is given by the following form:

$$\hat{y}_k(N|t_m) = y_{k-1}(N) + F_{k-1}(t_m)\Delta x_k^{\mathrm{RG}}(t_m|t_m) + \sum_{n=m}^{N_P} G_{k-1}(t_n)\Delta u_k(t_n) \tag{14}$$

It is straightforward to derive Eq. (14) from Eq. (12). Note that the state estimate $x_{k-1}(t|t)$ and $\Delta x_k^{RG}(t_m|t_m)$ are needed to construct Eq. (12) (for linearization) and to solve Eq. (13) for $\Delta u_k(\bullet)$ (using Eq. (14)), respectively.

4.2.3. State estimator

The state estimator is constructed separately for DH and RG in the form of the extended Kalman filter (EKF) for Eq. (10) and is given as

$$\begin{aligned} x_k(t+1|t) &= g(x_k(t|t), u_k(t)) \\ x_k(t|t) &= x_k(t|t-1) - K_k(t)(y_k(t) - c_k(t)x_k(t|t-1)) \end{aligned} \tag{15}$$

The observer gain $K_k(t)$ was obtained according to the EKF law using the process and measurement noise covariance matrices as the tuning factors (Minkler & Minkler, 1993). Using $x_k^{\mathrm{RG}}(t_m|t_m)$ and $x_{k-1}^{\mathrm{RG}}(t_m|t_m)$, $\Delta x_k^{\mathrm{RG}}(t_m|t_m) = x_k^{\mathrm{RG}}(t_m|t_m) - x_{k-1}^{\mathrm{RG}}(t_m|t_m)$ for Eq. (14) was estimated. The state estimator acts as a fixed-lag smoother at $t = N$ because the average product gas compositions are measured with one cycle of delay.

4.2.4. Implementation procedure

Over a DH–RG cycle, the following steps take turns in the repetitive control level:

[Step 1] *DH period*

$x_k^{\mathrm{DH}}(t|t)$ is estimated for $t = 1, \ldots, N$ using Eq. (15).

[Step 2] *Transition from DH to RG*

Initialize $x_k^{\mathrm{RG}}(1|0)$ by carrying over the coke deposit and bed temperature estimates in $x_k^{\mathrm{DH}}(N|N)$ to $x_k^{\mathrm{RG}}(1|0)$. Obtain the linearized model in Eq. (12) by linearizing Eq. (10) around $x_{k-1}^{\mathrm{RG}}(t|t)$ and $u_{k-1}(t-1)$, $t = 1, \ldots, N$.

[Step 3] *RG period*

Perform the state estimation using Eq. (15). Compute $\Delta x_k^{\mathrm{RG}}(t|t) = x_k^{\mathrm{RG}}(t|t) - x_{k-1}^{\mathrm{RG}}(t|t)$. Determine $\Delta u_k(t_m)$, $m = 1, \ldots, N_P$ according to Eqs. (13) and (14). Implement $T_k^{air}(t) = u_k(t) = u_{k-1}(t) + \Delta u_k(t)$ to the process.

[Step 4] *Transition from RG to DH*

Initialize $x_k^{\mathrm{DH}}(1|0)$ by transferring the coke deposit and bed temperature estimates in $x_k^{\mathrm{RG}}(N|N)$ to $x_k^{\mathrm{DH}}(1|0)$.

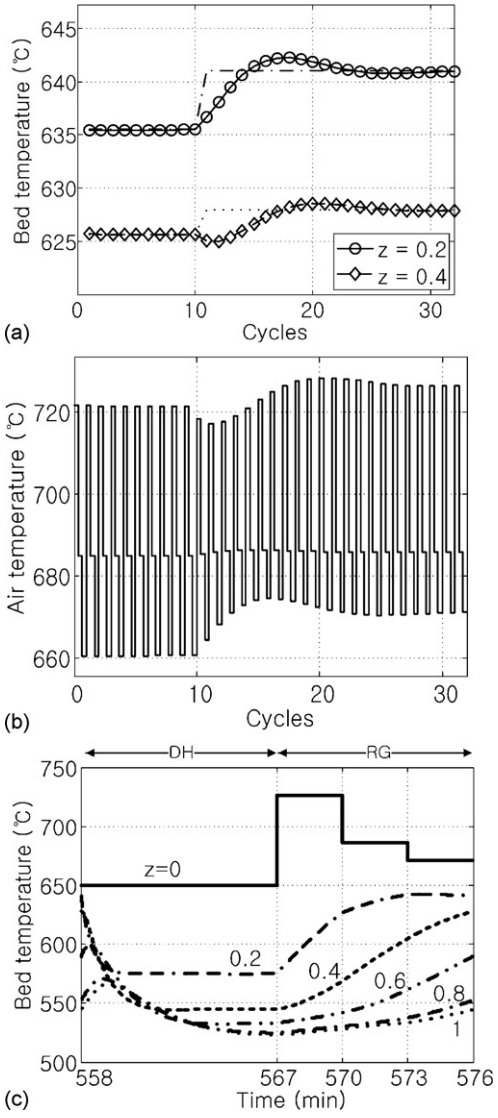

Fig. 8. Results of repetitive control for a set point change from [635.5 °C, 625.7 °C] to [641 °C, 628 °C]: (a) two controlled bed temperatures at the terminal time of RG operations, (b) input profiles, and (c) bed temperature trajectories in the new cyclic steady state.

4.3. Online cyclic steady state optimizer

The online optimizer, whenever invoked, determines T^{sp} and m^{air}, the target bed temperatures and the combustion air flow rate, respectively, that minimize the cost function under a cyclic steady state. The objective function is designed to be composed of a profit term by propylene production and cost terms by energy consumption to preheat the combustion air and catalyst deactivation by high bed temperature. The sign of the first term is taken to be negative for

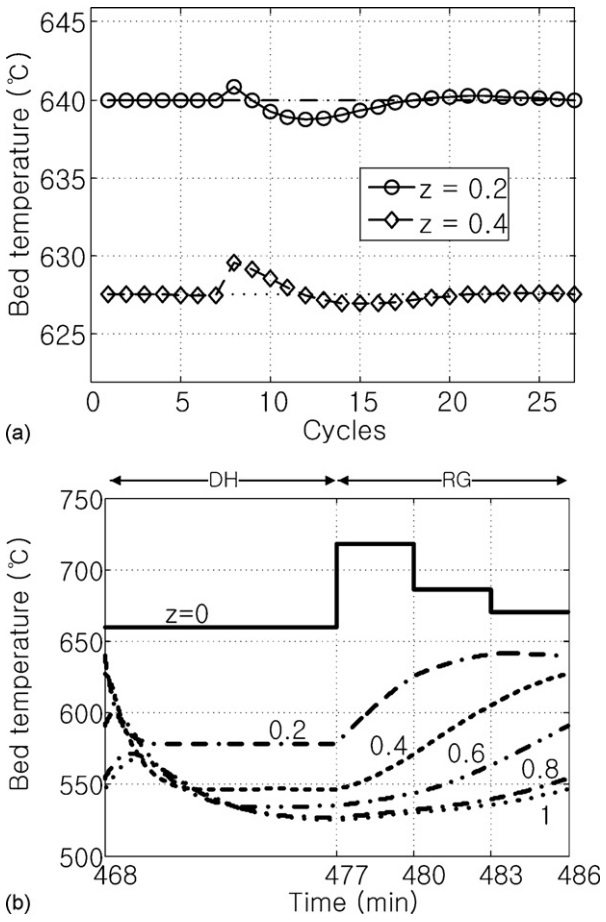

Fig. 9. Control performance against a step change in the propane inlet temperature during the DH operation (650 °C → 660 °C): (a) two controlled bed temperatures at the terminal time of RG operations and (b) bed temperature trajectories in the new cyclic steady state.

profit maximization during minimization of the objective function

$$\begin{aligned}
&\min_{T^{sp},m^{air}} J = -\alpha_1 m^p Y^p_{css} + \alpha_2 \sum_{t=1}^{N} c_{pg} m^{air} \left(T^{air}_{css}(t) - T_{amb}\right) \\
&+\alpha_3 \left(\max(0, T^{sp}_{z=0.2} - 500)\right)^2 + \|s\|^2_Q, \quad \alpha_i > 0, \quad Q > 0 \\
&\text{subject to} \quad \text{Eq. (10)} \\
&\begin{bmatrix} 615 \\ 600 \end{bmatrix} \le T^{sp} \le \begin{bmatrix} 720 \\ 690 \end{bmatrix} (^\circ\text{C}) \\
&10 \le \left|T^{sp}_{z=0.2} - T^{sp}_{z=0.4}\right| \le 30\,(^\circ\text{C}) \\
&90 \le m^{air} \le 120 \ (\text{kmol/min}) \\
&s = x^{\text{DH}}(0) - x^{\text{RG}}(N)
\end{aligned} \tag{16}$$

where T^{air}, T_{amb}, m^p, and Y^p represent the air temperature over a RG period, ambient temperature taken as 25 °C, propane mass flow rate, and average propylene yield over a DH period, respectively; α_i and the subscript *css* mean the unit price of the corresponding term and cyclic steady state, respectively. The summation in the second term is taken only over the RG period. The last term in J is to enforce the cyclic steady state condition, which is slackened by introducing a slack variable s defined the last equation in Eq. (16). Kawajiri and Biegler (2006) considered three different numerical approaches to enforce the cyclic steady state condition and evaluated their performances in an ordinary SMB process and also a PowerFeed process. In this study, the simultaneous single-discretization approach, where the initial state is updated using an optimization technique, was used. To solve the above constrained optimization, a sequential quadratic programming (SQP) method was used. In the programming, the gradient and the hessian are computed using the nominal model, while the objective function is measured from the virtual Catofin process as shown in Fig. 5.

4.4. Model parameter estimator

The model parameter estimator updates key parameters of the nominal model, whenever invoked, to best represent the process behaviour. In this study, the catalyst deactivation was assumed to be the most important process change and the model parameter estimator was designed to update the pre-exponent rate constants by minimizing the following quadratic objective on the prediction error:

$$\begin{aligned}
&\min_{\theta^i} V^i = \frac{1}{k_2 - k_1} \sum_{k=k_1}^{k_2-1} \sum_{t=1}^{N} \left\| y^{m,i}_k(t) - y^i_k(t;\theta^i) \right\|^2_{\bar{Q}}, \quad \bar{Q} > 0, \quad i=\text{DH, RG} \\
&\text{subject to } \theta^i_{\min} \le \theta^i \le \theta^i_{\max}
\end{aligned} \tag{17}$$

where $y^{m,i}_k(t)$ and $y^i_k(t;\theta^i)$ represent the measurement and model prediction of $y^i_k(t)$ based on θ^i, respectively.

Note that the catalyst deactivation has time-varying spatial distribution since it is affected by the bed temperature integrated over time. The nominal model was modified to have different pre-exponent rate constants at different collocation points to reflect this fact. With fresh catalysts, the axial profile of the bed temperature is monotonically decreasing under a cyclic steady state except some inversion during an initial time of the DH period as can be seen in Fig. 2. This causes the deactivation severer in the fore part of the bed and milder in the rear part of the bed. Once the fore part of the bed loses activity to a degree, then the reaction becomes active and catalyst deactivation is accelerated in the next part of the bed. As time elapses, the degree of activity loss becomes more and more uniform over the whole bed. To represent such behaviour succinctly, we devised a two parameter function as in Eq. (18), which is to be multiplied to each of the pre-exponent rate constants. In Fig. 7, sample profiles of $\xi(z)$ for different parameter values are shown

$$\xi(z) = \begin{cases} \frac{1}{2}\left(a + 1 + (1-a)\sin\left((-\pi/2d)(z+d)\right)\right) \\ 1 \qquad \text{if } z \ge 2d \end{cases}, \quad z \in [0,1] \tag{18}$$

Since there are four rate constants for the DH, $\theta^{\text{DH}} \triangleq [a_1 \ \cdots \ a_4 \ d_1 \ \cdots \ d_4]^T$. Likewise, $\theta^{RG} \triangleq [a_5 \ d_5]^T$.

It is true that Eq. (18) is only a rough description of the catalysts activity distribution in the real process. There may be appreciable mismatch between the reaction rate constants of the nominal model and the real process even with the best-fit parameter estimates. Nonetheless, both the repetitive controller and the optimizer can achieve highly precise tracking as well as the true minimum, respectively, overcoming model uncertainties since the controller performs the cycle-wise integral action and the optimizer searches for the minimum on the basis of the process measurements.

5. Simulation conditions

The sampling period was chosen to be 3 s resulting in total sampling instants of 360 with $t^{\text{RG}} = t^{\text{DH}} = 180$ over an entire cycle. The number control moments, N_P, (see Eq. (13)) was chosen as 3, and t_1, t_2, and t_3 were selected as 1, 60, and 120, respectively. This choice was made on the basis of numerous simulation studies, where the regulation performance was observed satisfactory

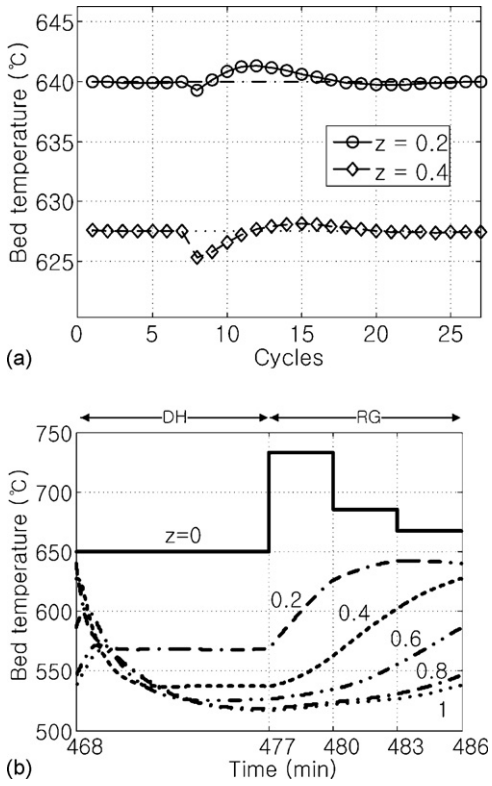

Fig. 10. Control performance against step changes in the pre-exponent constants of the reaction rates ($k_i \rightarrow 1.4k_i$, $i = 1, \ldots, 5$): (a) two controlled bed temperatures at the terminal time of RG operations and (b) bed temperature trajectories in the new cyclic steady state.

in almost all cases with $N_P = 3$, but not with $N_P = 1$ or 2. The following constraints were imposed on the MV movements for repetitive control:

$$600 \leq u(t) = T^{air}(t) \leq 750\,(^{\circ}\mathrm{C}) \tag{19}$$

In the virtual process, the case of catalyst deactivation is represented by multiplying all k_i 's by $1 - 0.5\exp(-2.4z)$.

6. Results and discussion

6.1. Performance of repetitive control

The performance of the controller has been investigated for three cases. In the first case, the temperature set point at the terminal time of the RG operation was changed from [635.5 °C, 625.7 °C], which is the output values of the cyclic steady state under the normal operating condition, to [641 °C, 628 °C] to observe the set point tracking performance. In the second case, the inlet temperature of propane during the DH operation was increased from 650 °C to 660 °C to verify the disturbance rejection performance. In the last case, the pre-exponent rate constants were increased by 1.4 times to investigate the zero offset performance overcoming the model uncertainty.

In Fig. 8, the responses of the bed temperatures at $z = 0.2$, 0.4 at the terminal time of the RG operations and the corresponding input changes to the set point change are shown. It can be observed from Fig. 8(a) that the bed temperatures are subject to some overshoot but settle on the respective set points in around 15 cycles of operation. Also it can be noted that the MV (air temperature) changes three times for each cycle as in Fig. 8(b) and the bed temperatures reach a new cyclic steady state as shown in Fig. 8(c).

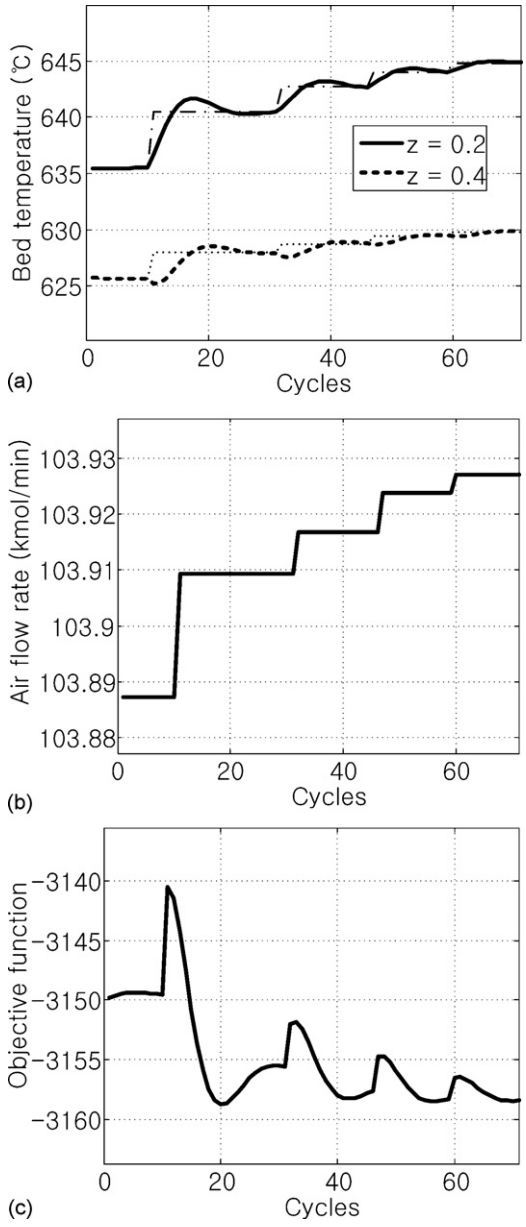

Fig. 11. Results of online optimization starting from an arbitrary open-loop state: (a) bed temperatures and their target values, (b) combustion air flow rate, and (c) objective function.

Fig. 9 depicts the output responses to a step change in the propane inlet temperature during the DH operation. As can be seen, the bed temperatures deviates from their respective set points for a while when the change starts, but the controller recovers the bed temperatures rapidly after a short transient.

In Fig. 10, the output responses to a step change in the rate constants are shown. In this case, too, the bed temperatures undergo some deviation from their respective set points but completely return to the set points in around 10 cycles of transient overcoming the large parameter error.

One of the interesting observations from the above simulations is that the resulting cyclic steady state air temperature has a decreasing trajectory with time. This tells that the time varying air temperature can minimize the quadratic objective in Eq. (13) more tightly than the constant air temperature can in the single input two output control problem.

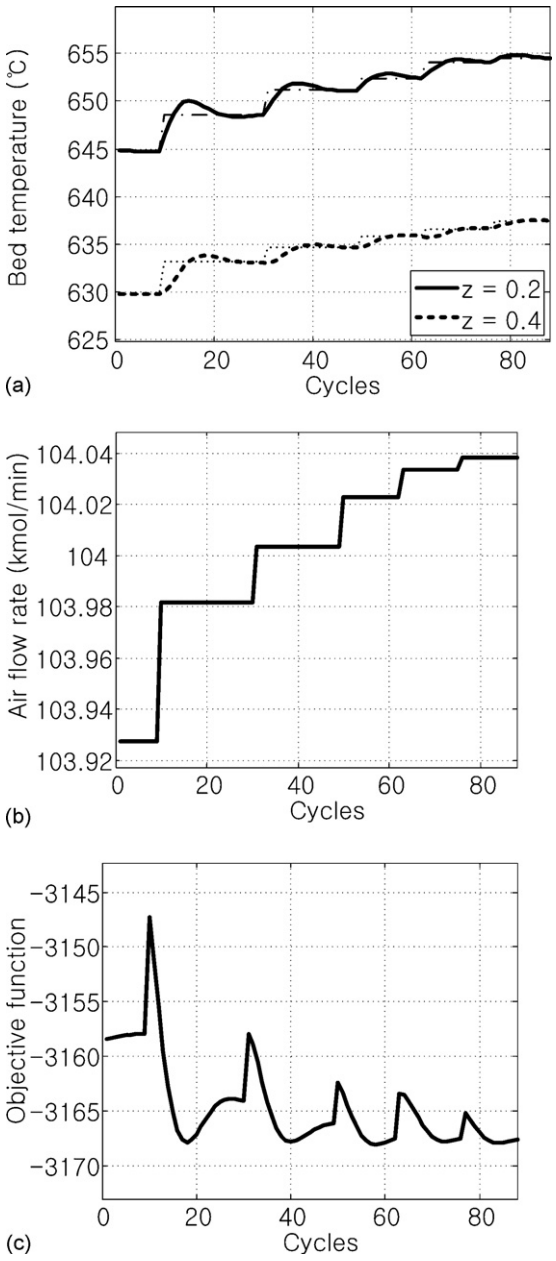

Fig. 12. Results of online optimization after the catalyst deactivation occurs: (a) bed temperatures and their target values, (b) combustion air flow rate, and (c) objective function.

6.2. Online optimization

The performance of the optimizing control system has been investigated for two cases. In the first case, the reactor was assumed to be initially at an arbitrary open-loop cyclic steady state and the optimizer steers the reactor to an optimum condition. In this case, the model parameter estimator was not invoked. In the second case, the optimum operation condition was assumed to be changed by catalyst deactivation, and the optimizer seeks for a new optimum condition from the previous operating condition determined in the first case. In the second case, the model parameter estimator plays an important role for both the repetitive controller and the online optimizer.

The simulation results for the first case are summarized in Fig. 11. It shows the response of the bed temperatures to their respective target values sent by the optimizer and the decrease of the objective function as the online optimization proceeds. The online optimizer calculates the new optimal target values once a cyclic steady state is reached on the basis of the nominal model and process measurements whereas the repetitive controller maneuvers the air temperature to attain the target values. Fig. 11(a) exhibits the controller performance with the bed temperature target values updated by the optimizer and Fig. 11(b) shows the combustion air flow rate update by the optimizer. The bed temperatures undergo a slight overshoot but are always settled on the target values within ten to twenty cycles. During this process, the cost function is decreased as shown in Fig. 11(c).

The simulation results for the second case are given in Fig. 12. It can be seen that the overall responses are similar to Fig. 11. Unlike in the previous case, however, θ^{DH} and θ^{RG} were recurrently updated during the optimization. One thing to note is that the bed temperatures are raised even higher from the values determined in the first case to compensate for the catalyst deactivation.

7. Conclusions

An online optimizing control system has been proposed for the Catofin propane process and its performance has been investigated numerically. A special feature of the Catofin process is that its operation is cyclic. In addition, a gradual catalyst deactivation requires periodic adjustment of the operating conditions, especially the initial bed temperatures for dehydrogenation operation, to maintain the propylene yield. To accommodate these features, the repetitive control technique based on a successively linearized model and an online cyclic steady state optimizer have been proposed. To provide the controller and optimizer with the most recent process information, a model parameter estimator was built, too, to chase the process change. The nominal model that underlies all these modules was derived from a first-principle reactor model by applying the cubic spline collocation method and forward-difference discretization.

The numerical study has shown that the proposed optimizing control works quite satisfactorily, readily seeking for optimum conditions in a relatively short transient for different scenarios in the process change. Such performance is mostly attributed to the repetitive controller which enables the process to settle on the set points commanded by the optimizer in a short period of time with a minimum overshoot coping with model uncertainties.

Acknowledgements

This work was supported by grant No. 2005-E-ID03-P-02-0-000 from Korea Research Foundation program of the Korea Energy Management Corporation. W. Won would like to acknowledge the financial support from the Seoul Metropolitan Government.

References

ABB (2008). http://www02.abb.com/GLOBAL/NOOFS/noofs187.nsf/viewunid/494CDF435B2EE22DC12569EE0036977A/$file/CATOFIN.pdf.

Abel, S., Mazzotti, M., Erdem, G., Morari, M., & Morbidelli, M. (2004). Optimizing control of simulated moving beds: Linear isotherm. *Journal of Chromatography A*, *1033*, 229–239.

Bhasin, M. M., McCaina, J. H., Vora, B. V., Imai, T., & Pujad, P. R. (2001). Dehydrogenation and oxydehydrogenation of paraffins to olefins. *Applied Catalysis A: General*, *221*, 397–419.

Erdem, G., Abel, S., Morari, M., Mazzotti, M., Morbidelli, M., & Lee, J. H. (2004). Automatic control of simulated moving beds. *Industrial & Engineering Chemistry Research*, *43*, 405–421.

Froment, G. F., & Bischoff, K. B. (1990). *Chemical reactor analysis and design* (2nd ed.). New York: Wiley.

Hara, S., Yamamoto, Y., Omata, T., & Nakano, N. (1988). Repetitive control system: a new type servo system for periodic exogenous signals. *IEEE Transactions AC*, *33*, 659–668.

Jiang, L., Biegler, L. T., & Fox, V. G. (2003). Simulation and optimization of pressure-swing adsorption systems for air separation. *American Institute of Chemical Engineers Journal*, *49*(5), 1140–1157.

Jiang, L., Fox, V. G., & Biegler, L. T. (2004). Simulation and optimal design of multiple-bed pressure swing adsorption systems. *American Institute of Chemical Engineers Journal*, *50*(11), 2904–2917.

Kawajiri, Y., & Biegler, T. (2006). Optimization strategies for simulated moving bed and powerfeed processes. *American Institute of Chemical Engineers Journal*, *52*(4), 1343–1350.

Kim, Y. G., Lee, H. S., & Song, Y. S. (1980). A study on dehydrogenation of propane. *Korean Journal of Chemical Engineering*, *18*, 11–19.

Lee, J. H., Natarajan, S., & Lee, K. S. (2001). A model-based predictive control approach to repetitive control of continuous processes with periodic operations. *Journal of Process Control*, *11*, 195–207.

Mickley, H. S., Nestor, J. W., & Gould, L. A. (1965). A kinetic study of the regeneration of a dehydrogenation catalyst. *Canadian Journal of Chemical Engineering*, 61–68.

Minkler, G., & Minkler, J. (1993). *Theory and application of Kalman filtering*. Palm Bay: Magellan.

Natarajan, S., & Lee, J. H. (2000). Repetitive model predictive control applied to a simulated moving bed chromatography system. *Computers & Chemical Engineering*, *24*, 1127–1133.

Nijhuis, T. A., Tinnemans, S. J., Visser, T., & Weckhuysen, B. M. (2004). Towards real-time spectroscopic process control for the dehydrogenation of propane over supported chromium oxide catalysts. *Chemical Engineering Science*, *59*, 5487–5492.

Pena, J. A., Monzon, A., & Santamaria, J. (1993). Coking kinetics of fresh and thermally aged commercial Cr2O3/Al2O3 catalyst. *Applied Catalysis A*, *101*, 185–198.

Qin, S. J., & Badgwell, T. A. (2003). A survey of industrial model predictive control technology. *Control Engineering Practice*, *11*, 733–764.

Reuters, (2008). http://www.reuters.com/article/press Release/idUS106137+10-Oct-2008+BW20081010.

Yun, W., & Lee, K. S. (2007). The use of cubic spline and far-side boundary condition for the collocation solution of a transient convection-diffusion problem. *Korean Journal of Chemical Engineering*, *24*, 204–208.